RSC Advances

ROYAL SOCIETY OF CHEMISTRY

www.rsc.org/advances

Graphical Abstract:

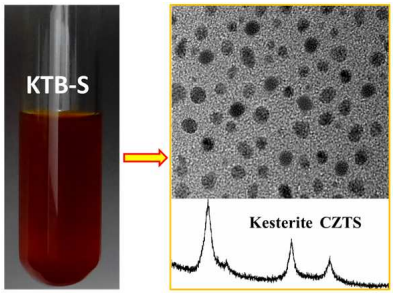

High quality CZTS nanocrystals were facilely synthesized. The uniqueness is the use of KTB as sulfur activating agent and stabilizer.

Journal Name

RSCPublishing

COMMUNICATION

Facile non-injection synthesis of high quality CZTS nanocrystals

Cite this: DOI: 10.1039/xoxxoooooox

Yuanhao Gao,[*a] Huaizhi Yang,[a] Yange Zhang,[a] Jing Li,[a] Hongxiao Zhao,[a] Jianjun Feng,[a] Jintao Sun[a] and Zhi Zheng[*a]

Received ooth January 2012,
Accepted ooth January 2012

DOI: 10.1039/xoxxoooooox

www.rsc.org/

We present a facile, non-injection synthesis of high quality CZTS nanocrystals by using simple inorganic salts, sulfur powders and $(CH_3)_3COK$ (KTB) as precursors. The uniqueness and creation is the utilization of KTB as sulfur activating agent and stabilizing surfactant agents.

High-quality semiconductor nanocrystals are defined as nano-scale crystals that have high composition controllability, desired particle size, monodispersity, narrow size distribution, high crystallization, optimum band gap, etc. How to synthesize high-quality semiconductor nanocrystals has long been an important topic in the field of materials chemistry due to the fundamental research interest and industrial applications.[1-3] Recently, Cu_2ZnSnS_4 (CZTS) nanocrystals, as a promising absorber material for the low-cost and high performance photovoltaics, have attracted considerable attention.[4-9] Compared with most of other absorber materials for photovoltaic devices, it has a number of advantages, such as the large absorption coefficient ($>10^4$ cm^{-1}), near-optimum direct band gap (1.4–1.6 eV), non-toxicity and earth elemental abundance.[10,11]The reported power conversion efficiency (PCE) of CZTS-based solar cells has increased from 0.66% to 11.1% very recently. Moreover, this PCE can be further improved through optimizing the fabrication process, since Shockley–Queisser photon balance calculations have shown that the theoretical single junction PCE limit for CZTS is 32.2%.[5,6.12,13] Advances in the synthesis of high quality CZTS nanocrystals have opened up a new possible route to further improve the CZTS-based solar cells. Until now, monodisperse CZTS nanocrystals have been mainly synthesized based on the reaction between metal salts and various sulfur sources [4–6] or by thermal decomposition of single-source precursors such as metal thiolate[14–17] and metal dithiocarbamate complexes[18–21] in suitable high-boiling-point solvents. Alkanethiols and fatty amines are the most commonly used solvents, in which the formation of unwanted binary and ternary products is suppressed while quaternary CZTS nanocrystals of high purity are obtained. In above studies, the hot injection technique is often employed to produce a "burst nucleation" event, which is a crucial factor for the narrow size distribution of the products. Also, a high reaction temperature of ~300 °C is required to fully decompose all the complex precursors, otherwise the premature decomposition can result in unwanted phases (e.g. SnS_2, Cu_2S and Cu_3SnS_4). However, the high reaction temperature and the hot injection process often lead to a complicated manipulation, which limit the application in the scaled-up manufacture. Recently, Chesman et al.[22] presented a non-injection synthesis of kesterite CZTS nanocrystals through the selective use of the binary sulfur precursors ($Zn(EtXn)_2$ and DDT) and surfactants mixture (OA and DDT). But, this approach requires an extremely careful design of the $Zn(EtXn)_2$ complex, and also employs toxic precursors and surfactants. Hence, it is highly desirable to develop a rational method to prepare high quality CZTS nanocrystals using simple operation technique, non-toxic precursors and solvents.

In this work, we report a facile, non-injection synthesis of the kesterite CZTS nanocrystals by reacting simple Cu(II), Zn(II) and Sn(II) inorganic salts with sulfur powders in an ethanol solution of $(CH_3)_3COK$ (KTB). Here, KTB was used as both the sulfur activating agent and stabilizing surfactant agent.

In a typical synthetic process, S powders (4 mmol) were first dissolved into the ethanol solution of KTB (1.5 M, 20 mL) at 80 °C in 30 min. In this step, S powder was activated by KTB forming reactive polysulfide precursors, and the solution colour changed from yellow to orange, then to red. Next, a 10 mL of ethanol solution containing 2.0 mmol $CuCl_2{\cdot}2H_2O$, 1.0 mmol $ZnCl_2{\cdot}2H_2O$ and 1.0 mmol $SnCl_2{\cdot}2H_2O$ was added drop by drop into the red polysulfide precursors solution, resulting in sensorial intermediate nanocrystal formation. In this stage, the Cu^{2+} and Sn^{2+} ions had been changed into Cu^+ and Sn^{4+} through oxidation–reduction reactions, since tin(II) chloride is a strong reducing agent. After heating and stirring for 1 h at 150 °C under an inert atmosphere, the mixture turned into blackish slurry. The crude CZTS nanocrystals were obtained by drying the blackish slurry in vacuum oven at 150 °C for 30 min and then raising to 250 °C for 2 h for further growth. The powdery CZTS nanocrystals were purified by adding ethanol to remove the excess KTB, and subsequent centrifugation and washing with distilled water for several times. The obtained CZTS nanocrystals (yield >80%) meet all these requirements of high quality nanocrystals, which have been confirmed by powder X-ray diffraction (XRD), Raman spectrometer, transmission electron microscopy (TEM), energy dispersive X-ray spectroscopy (EDS), X-ray photoelectron spectroscopy (XPS) and UV–vis absorption spectroscopy.

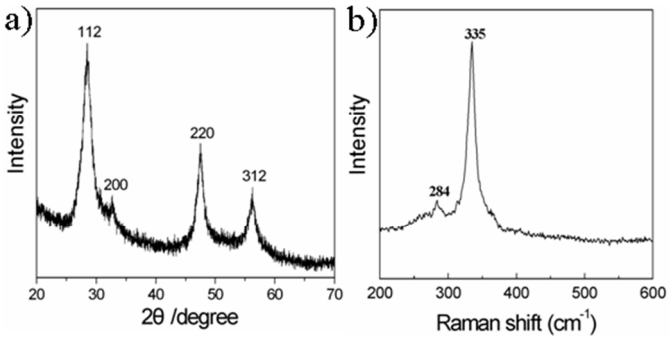

Fig.1 XRD pattern (a) and Raman spectra (b) of CZTS nanocrystals

Fig.1a shows the XRD pattern of the as-synthesized CZTS nanocrystals, where the observed diffraction peaks match well with those of the expected kesterite CZTS (JCPDS 26–0575). The average nanocrystal size estimated to be 7.6 nm by the Debye-Scherrer equation from full width at half maximum of the (112) and (220) peaks. Because the possible sulfides by-products, e.g. ZnS, SnS_2 and Cu_2SnS_3 have similar XRD patterns overlapping with that of CZTS,[23, 24] Raman spectra were used to provide a more definitive structure assignment. As shown in **Fig.1b**, only two Raman peaks at 335 and 284 cm^{-1} are detected, which is in good agreement with the reported CZTS modes at 337 and 286 cm^{-1}.[20, 21] No other characteristic peaks of impurities are observed, such as ZnS (351 and 274 cm^{-1}), Cu_3SnS_4 (318, 348, and 295 cm^{-1}), SnS_2 (315 cm^{-1}), and so on.[20, 21, 23, 24] Thus, we are confident that the nanocrystals are CZTS rather than any other sulfide phases. Moreover, XPS analyses indicate the nanocrystals are composed of Cu, Zn, Sn, and S, and the oxidation states of all four elements are consistent with those of CZTS (Fig.S1, ESI†).

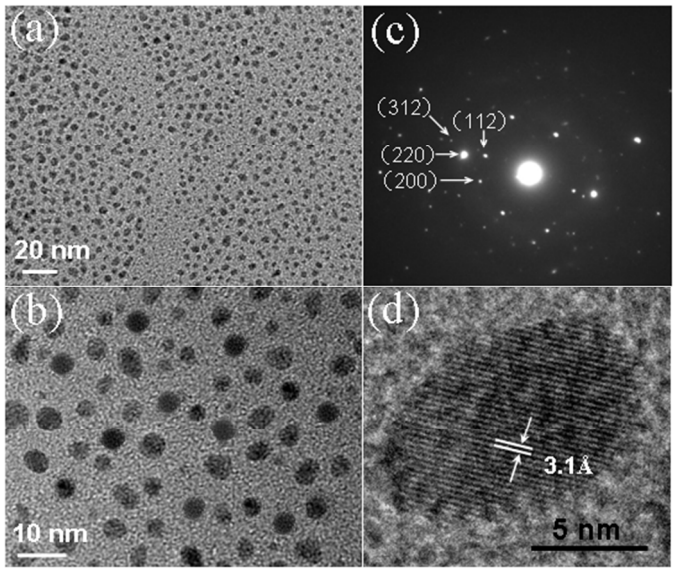

Fig. 2 TEM (a, b) and SAED (c) and HRTEM (d) images of CZTS nanocrystals.

Fig. 2 are the transmission electron microscopy (TEM) and selected area electron diffraction (SAED) images of as-synthesized CZTS nanocrystals. Lower-magnification TEM images (Fig. 2a and 2b) exhibit that the CZTS nanocrystals are nearly perfectly spherical and highly monodisperse with most of the nanocrystals in the range of 5–8 nm (corresponding size distribution plot is shown in Fig. S2, ESI†). The diffraction spots of the (112), (200), (220) and (312) planes in the SAED pattern (Fig. 2c) indicates that the CZTS nanocrystals are highly crystallized. The HRTEM image (Fig. 2d) shows lattice spacing of d = 3.1 Å corresponding to the (112) lattice plane of kesterite CZTS. The average composition of the CZTS nanocrystals determined by EDS analysis is $Cu_{1.84}Zn_{1.14}Sn_{0.91}S_4$ (Fig. S3, ESI†). The CZTS nanocrystals are slightly Cu, Sn poor and Zn rich. As the reported most efficient photovoltaic devices are Zn rich and Cu, Sn deficient (Zn/Sn=1.1–1.4, Cu/(Zn+Sn)=0.8–0.9),[8, 25] it is evident that our CZTS nanocrystals with this metal composition (Zn/Sn=1.25, Cu/(Zn+Sn)=0.90) can be suitable for photovoltaic devices.

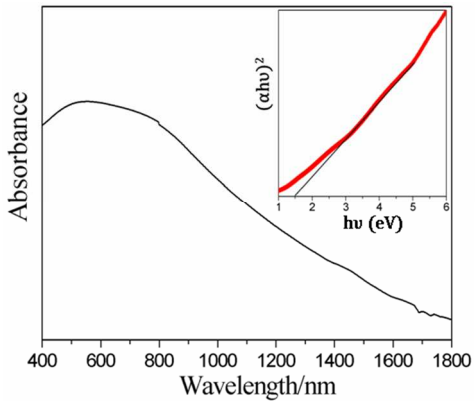

Fig. 3 Room temperature optical absorption spectrum of CZTS nanocrystals. The inset shows an obtained band gap of 1.5 eV.

UV-vis absorption spectroscopy is used to evaluate the optical absorption properties of the CZTS nanocrystals (**Fig. 3**). The direct optical band-gaps of the resulting CZTS nanocrystals is determined through the extrapolation of $(\alpha hv)^2$ *vs. hv*, where α is the absorption coefficient and *hv* is the photon energy. We find that the direct optical band-gap of the CZTS is ~1.5 eV and consistent with the literature values of 1.4–1.6 eV.[10, 11] This value is near the optimum for photovoltaic solar conversion in a single-band-gap device.

It is well known that the precursors and surfactants used in the CZTS synthesis have strongly influence on the initial nucleation, subsequent growth and crystallographic phase of the final CZTS nanocrystals. Apparently, the key to our controlled synthesis of CZTS nanocrystals is the utilization of KTB. Firstly, the KTB was used as sulfur activation agent to produce active polysulfide precursors. In Zou's work, octadecene (ODE) has been used as sulfur activation agent for the synthesis of CZTS nanocrystals in which sulfur dissolved in octadecene to produce active orange polysulfide precursor solution (ODE-S).[4] In this study, KTB is relatively environmentally friendly and economical, which can be easily decomposed in water or dissolved in ethanol for recycle. Importantly, KTB is very efficient for sulfur activation to generate active polysulfide precursors. To obtain an active polysulfide precursor solution, only 30 min heating time was enough when a mixture of 4 mmol of S and 10 mL of KTB solution (1.5M) was heated at 80 °C. While the solution color changed from yellow to orange and then to red color, and no S precipitation was observed in the final red polysulfide precursor solution after overnight storage (Fig. S4, ESI†). The color change in the preparation of the polysulfide precursor solution was reminiscent of the formation of polysulfide ions (S_n^{2-}) in the well-known reaction between S and NaOH aqueous solution. With increasing n, the S_n^{2-} solution colour turns from yellow to orange and then to red. Moreover, preliminary results from orange ODE-S precursor solution showed the possible existence of $(C_{18}H_{35})_2S_5$ and $(C_{18}H_{35})_2S_{10}$.[4] Considering to the strong alkaline activity of KTB similar to NaOH, we propose that the red polysulfide precursors in our work contains polysulfide ions (S_n^{2-}),

although more detailed investigations are needed to accurately identify the active species in the prepared red polysulfide precursors. We believe the existence of polysulfide ions (S_n^{2-}) with long S chains makes the red polysulfide precursors more reactive than its yellow and orange counterparts, as the S−S bond in long sulfur chains is much weaker and active due to electron delocalization along the whole S_n^{2-} chain. Thus, the red polysulfide precursors (S_n^{2-}) are sufficiently reactive to induce an initial "burst nucleation", which is a crucial factor for the narrow size distribution growth of the CZTS nanocrystals.

Second, the KTB was used as stabilizing surfactant in present fabrication of well monodisperse CZTS. Generally, the selection of appropriate stabilizing surfactant molecules having optimum binding strength and steric bulkiness is critical for the synthesis of small nanocrystales or quantum dots at lower temperature. In this synthesis, KTB as a stabilizing surfactant molecule is very effective in controlling the nucleation and growth of CZTS nanocrystals, possibly due to its steric bulkiness and appropriate affinity for metal ions. As a result, the obtained CZTS nanocrystals display nearly perfectly spherical crystalline particles with the diameter of 5−8 nm, which clearly demonstrates the suppression of the Ostwald ripening process ("defocusing") in the current synthetic procedure. The absence of "defocusing" means that the narrow size distribution corresponds to the largest size achievable at the given growth temperature of 250 °C. In contrast, when KTB was substituted with NaOH in our synthetic procedure, two coexisting CZTS phases (wurtzite and kesterite) were found simultaneously (Fig. S5, ESI†), and most of the CZTS nanocrystals were nanoplates or nanorods with large sizes (Fig. S6, ESI†). This result indicates that the KTB is indeed determining factor for the phase-controlled synthesis of kesterite-type CZTS nanocrystals. Previously, it has been proved that the crystallographic phase of the final CZTS nanocrystals is influenced by the reaction rate between the metal precursor and S precursor, which can be tuned by adding different surfactant agents.[26, 27] More work is still needed to fully understand the growth mechanism of kesterite CZTS nanocrystals in the current synthetic procedure, including the effect of KTB on the reaction rates between the metal precursors and polysulfide precursors, the composition tuning through the precursor ratio and so on.

As a final remark, the heating temperature is a key for the growth of CZTS nanocrystals. Several control experiments at different heating temperature were performed and revealed a few interesting changes. When the heating temperature is below 200°C, only unidentified black precipitates resulted (Fig. S7a, ESI†). Typically, the well-defined CZTS nanocrystals were prepared at the heating temperature of 250°C (see Fig. 1 and Fig. 2). Further increasing temperature to 300°C, no obvious intrinsic structure changes were observed, however, the exterior morphology became irregular in bigger scale with a few of agglomerates(Fig. S7b,c,d, ESI†).

In conclusion we have presented a convenient chemical synthesis of kesterite CZTS nanocrystals by reacting metal salts and sulfur powders in KTB ethanol solution. KTB functions as both the sulfur activating agent and stabilizing surfactant agent. A series of rational investigations show that the high quality kesterite CZTS nanocrystals with high crystallization, monodispersity, narrow size distribution and desired metal composition control are successfuly achieved. And this convenient chemical approach to high quality CZTS nanocrystals may facilitate the scaled-up manufacture.

Acknowledgements

This work was supported by the National Natural Science Foundation of China (21271152, 21273192, 61106125), Innovation Scientists and Technicians Troop Construction Projects of Henan Province (Grant No. 104100510001), the Program for New Century Excellent Talents in University (grant number NCET-08-0665), and the Program for Science & Technology Innovation Talents in Universities of Henan Province (2011HASTIT029).

Notes and references

[a] Key Laboratory of Micro-Nano Materials for Energy Storage and Conversion of Henan Province and Institute of Surface Micro and Nano Materials, Xuchang University, Henan 461000, China. E-mail: gyh-2007@sohu.com; zhengzhi99999@gmail.com

†Electronic Supplementary Information (ESI) available: XPS and EDS spectra for CZTS nanocrystals; Size distribution plot for CZTS nanocrystals; XRD pattern and TEM image of CZTS nanocrystals obtained in NaOH ethanol solution; XRD pattern, TEM image and SAED of samples obtained at different heating temperature. Color photograph of the polysulfide precursor solution. See DOI: 10.1039/c000000x/

1 X. G. Peng, L. Manna, W. D. Yang, J. Wickham, E. Scher, A. Kadavanich, A. P. Alivisatos, *Nature*, 2000, **404**, 59−61.
2 L. Li, H. F. Qian, J. C. Ren, *Chem.Commun.*, 2005, 528–530.
3 J. S. Owen, E. M. Chan, H. T. Liu, A. P. Alivisatos, *J. Am. Chem. Soc.*, 2010, **132**, 18206–18213.
4 Y. Zou, X. Su, J. Jiang, *J. Am. Chem. Soc.*, 2013, **135**, 18377−18384.
5 Q. Guo, H. W. Hillhouse, R. Agrawal, *J. Am. Chem. Soc.*, 2009,**131**, 11672–11673.
6 C. Steinhagen, M. G. Panthani, V. Akhavan, B. Goodfellow, B. Koo, B. A. Korgel, *J. Am. Chem. Soc.*, 2009, **131**, 12554–12555.
7 Q. Guo, H. W. Hillhouse, R. Agrawal, *J. Am. Chem. Soc.*, 2009, **131**, 11672–11673.
8 H. P. Zhou, W. C. Hsu, H. S. Duan, B. Bob, W. B. Yang, T. B. Song, C. J. Hsu, Y. Yang, *Energy Environ. Sci.*, 2013, **6**, 2822–2838.
9 W. C. Liu, B. L. Guo, X. S. Wu, F. M. Zhang, C. L. Mak, K. H. Wong, *J. Mater. Chem. A*, 2013, **1**, 3182–3186.
10 D. B. Mitzi, O. Gunawan, T. K. Todorov, K. Wang, S. Guha, *Sol. Energy Mater. Sol. Cells*, 2011, **95**, 1421–1436.
11 K. Ramasamy, M. A. Malik and P. O'Brien, *Chem. Commun.*, 2012, **48**, 5703–5714.
12 T. Washio, T. Shinji, S. Tajima, T. Fukano, T. Motohiro, K. Jimbo, H. Katagiri, *J. Mater. Chem.*, 2012, **22**, 4021–4024.
13 D. A. R. Barkhouse, O. Gunawan, T. Gokmen, T. K. Todorov, D. B. Mitzi, *Prog. Photovoltaics*, 2012, **20**, 6−11.
14 X. Lu, Z. Zhuang, Q. Peng, Y. Li, *Chem. Commun.*, 2011, **47**, 3141.
15 A. Singh, H. Geaney, F. Laffir, K. M. Ryan, *J. Am. Chem. Soc.*, 2012, **134**, 2910–2913.
16 H. C. Liao, M. H. Jao, J. J. Shyue, Y. F. Chen, W. F. Su, *J. Mater. Chem. A*, 2013, **1**, 337−341.
17 J. Chang, E. R. Waclawik, *CrystEngComm*, 2013, **15**, 5612−5619.
18 A. S. R. Chesman, J. van Embden, N. W. Duffy, N. A. S. Webster, J. J. Jasieniak, *Cryst. Growth Des.*, 2013, **13**, 1712−1720.
19 A. Khare, A. W. Wills, L. M. Ammerman, D. J. Norris, E. S. Aydil, *Chem. Commun.*, 2011, **47**, 11721−11723.
20 M. D. Regulacio, C. Ye, S. H. Lim, M. Bosman, E. Ye, S. Chen, Q. H. Xu, M. Y. Han, *Chem. Eur. J.*, 2012, **18**, 3127−3131.
21 C. Zou, L. J. Zhang, D. S. Lin, Y. Yang, Q. Li, X. J. Xu, X. A. Chen, S. M. Huang, *CrystEngComm*, 2011, **13**, 3310-3313.
22 A. S. R. Chesman, N. W. Duffy, S. Peacock, L. Waddington, N. A. S. Websterbc, J. J. Jasieniak, *RSC Adv.*, 2013, **3**, 1017–1020.

23 P. A. Fernandes, P. M. P. Salome, A. F. da Cunha, *Thin Solid Films*, 2009, **517**, 2519–2523.
24 A. J. Cheng, M. Manno, A. Khare, C. Leighton, S. A. Capmbell, E. S. Aydil, *J. Vac. Sci. Technol. A*, 2011, **29**, 05120–051214.
25 H. Katagiri, K. Jimbo, M. Tahara, H. Araki, K. Oishi, *Mater. Res. Soc. Symp. Proc.*, 2009, **1165**, M04–01.
26 H. Zhong, S. S. Lo, T. Mirkovic, Y. Li, Y. Ding, Y. Li, G. D. Scholes, *ACS Nano*, 2010, **4**, 5253–5262.
27 T. Kuzuya, Y. Hamanaka, K. Itoh, T. Kino, K. Sumiyama, Y. Fukunaka, S. Hirai, *J. Colloid Interface Sci.*, 2012, **388**, 137-143.

